Journal of Power Sources 216 (2012) 237–248

Contents lists available at SciVerse ScienceDirect

Journal of Power Sources

journal homepage: www.elsevier.com/locate/jpowsour

Integrated thermal and energy management of plug-in hybrid electric vehicles

Mojtaba Shams-Zahraei [a,*], Abbas Z. Kouzani [a], Steffen Kutter [b], Bernard Bäker [b]

[a] School of Engineering, Deakin University, Waurn Ponds, Victoria 3216, Australia
[b] Institute of Automotive Technology Dresden – IAD, Dresden University of Technology, 01062 Dresden, Germany

HIGHLIGHTS

- PHEVs' optimal energy management strategy (EMS) is highly influenced by temperature.
- DP algorithm considers both battery charge and engine temperature state variables.
- Optimal charge depletion trajectory represents an optimal engine temperature trajectory.
- Real-time sub-optimal EMS can be realised by following the optimal charge trajectory.

ARTICLE INFO

Article history:
Received 7 March 2012
Received in revised form
11 May 2012
Accepted 21 May 2012
Available online 27 May 2012

Keywords:
Energy management strategy
Temperature
Thermal management
Plug-in hybrid electric vehicle
Optimal control
Dynamic programing

ABSTRACT

In plug-in hybrid electric vehicles (PHEVs), the engine temperature declines due to reduced engine load and extended engine off period. It is proven that the engine efficiency and emissions depend on the engine temperature. Also, temperature influences the vehicle air-conditioner and the cabin heater loads. Particularly, while the engine is cold, the power demand of the cabin heater needs to be provided by the batteries instead of the waste heat of engine coolant. The existing energy management strategies (EMS) of PHEVs focus on the improvement of fuel efficiency based on hot engine characteristics neglecting the effect of temperature on the engine performance and the vehicle power demand. This paper presents a new EMS incorporating an engine thermal management method which derives the global optimal battery charge depletion trajectories. A dynamic programming-based algorithm is developed to enforce the charge depletion boundaries, while optimizing a fuel consumption cost function by controlling the engine power. The optimal control problem formulates the cost function based on two state variables: battery charge and engine internal temperature. Simulation results demonstrate that temperature and the cabin heater/air-conditioner power demand can significantly influence the optimal solution for the EMS, and accordingly fuel efficiency and emissions of PHEVs.

1. Introduction

Plug-in hybrid electric vehicles (PHEVs) benefit from the features of both conventional hybrid electric vehicles (HEVs) and electric vehicles (EVs) by having a large battery pack which can be recharged when plugged into an electric power source. PHEVs offer a viable solution for transportation in which part of the required fossil fuel is replaced with electricity, before full electrification of vehicles becomes mature [1]. Moreover, PHEVs can address concerns about EVs' recharging time and range anxiety.

Available charge in PHEVs' energy storage system (ESS), generally a battery pack, adds more flexibility to the EMS of PHEVs in distributing load between the engine and ESS compared to conventional HEVs. A charge management strategy should be incorporated into the EMS of PHEVs. The charge management strategy in PHEVs defines how to share available ESS energy during a journey to optimally utilize it to improve the performance of the vehicle. The simplest charge management strategy for PHEVs is aggressive charge depletion until the batteries are depleted to their minimum state of charge (SOC) threshold. Then, the vehicle operates like a conventional HEV in a charge sustained (CS) mode. For extended-range electric vehicles (EREVs) in which both the ESS and electric motor of the PHEV are capable of providing maximum power demand of the powertrain, it is possible to run the vehicle in the electric vehicle (EV) mode. The maximum range which can be covered in the EV mode for a standard drive cycle is called all

* Corresponding author. Tel.: +61 3 522 72818, +61 430049876 (mobile); fax: +61 3 522 72167.
E-mail addresses: mshams@deakin.edu.au (M. Shams-Zahraei), kouzani@deakin.edu.au (A.Z. Kouzani), kutter@iad.tu-dresden.de (S. Kutter), baeker@iad.tu-dresden.de (B. Bäker).

0378-7753/$ – see front matter © 2012 Elsevier B.V. All rights reserved.
doi:10.1016/j.jpowsour.2012.05.055

electric range (AER). When the vehicle's power demand trajectory is unknown, the advantage of the AER followed by CS strategy (AER-CS) is the complete consumption of the relatively cheaper stored electric energy before the vehicle reaches its destination with available recharging facilities. A more sophisticated EMS, known as blended mode, is a controlled charge depletion strategy that benefits from the combined use of the available charge in the ESS and the engine energy simultaneously during the journey. Hence, the battery energy could improve load levelling in the hybrid system, more efficiently.

The classification of the EMS for HEVs and PHEVs is well outlined in the literature [2–6]. Many of the approaches that have been developed for the EMS of HEVs are also equally applicable to PHEVs. Other distinct approaches can be also found in the literature for developing a blended mode charge management; these approaches are formulated based on the architecture and components sizing of a specific PHEV [7–15]. Sharer et al. selected different engine-ignition power thresholds for different journey distances in a rule based EMS [15]. Gong et al. suggested drive cycle modelling using the global positioning system (GPS) and the geographical information system (GIS), and used it for developing a deterministic dynamic programming EMS [11]. Moura et al. applied a stochastic dynamic programming method to optimize a power split map for a probabilistic distribution of drive cycles, rather than a single drive cycle for a series-parallel PHEV [12].

A priori knowledge of the vehicle power demand trajectory has been proven to be essential for the development of optimal EMSs and especially for the charge management of PHEVs in a blended mode operation. The benefit of having a large battery on board could be sacrificed by reaching the destination with surplus electric energy. That is, a blended mode EMS could deteriorate the performance of a PHEV when compared with a simple AER-CS, if defined based on an inaccurate driving scenario prediction. Noise factors affecting the power demand and performance of different components of a PHEV, as well as the velocity trajectory need to be taken into account to predict a realistic power trajectory. These noise factors consist of (i) traffic diversity and aggressive driving, (ii) road grade, (iii) wind, (iv) battery ageing, and (v) ambient temperature. In this paper, it is assumed that the vehicle's power cycle, considering the noise factors, is predicted by the approach described in the authors' previous works [13,14]. In brief, since the majority of commuters use their vehicles on the same routes in a regular basis, by means of using historic velocity trajectories, GPS feedback, and a library of daily repetitive commutes, the power cycle is predictable with enough accuracy for PHEVs' charge management. The historic information about driving pattern for a known commute helps predict traffic pattern, aggressive driving factor, road grade, and battery ageing. On the other hand, daily wind, temperature, and humidity forecast information is required to consider the influence of such factors on the vehicle load and performance.

Among all the noise factors, temperature has the most complex effect on both power cycle prediction and vehicle performance. Temperature alters the aerodynamic force by affecting the air viscosity and density. Also, air-condition (AC) and cabin heating significantly increase the power demand of the vehicle. Since two energy sources exist in PHEV architecture, performance of PHEV components is more sensitive to temperature fluctuations. Cold engine operation deteriorates fuel consumption and pollution of the vehicle [16,17]. When the vehicle is controlled by a blended mode charge management strategy, the engine on/off shifting occurs more frequently, and the engine cools down when vehicle operates in the EV mode. The all electric range followed by charge sustained mode EMS for EREV intrinsically solves this issue as the operation of EREV is similar to that of a HEV during the CS mode. Cold engine operation, however, should be investigated when dealing with the blended mode EMS. The fuel efficiency of a vehicle drops substantially when the AC's compressor load is included. The all electric range could be decreased by 38% on a repeated EPA urban dynamometer driving schedule (UDDS) with 3 kW accessory load on a midsized PHEV [18]. Furthermore, when hot water is unavailable from the engine coolant during the EV mode or the AER, the power demand of the cabin electric heater and windscreen demister is even higher than AC. Assuming the absolute difference between comfort and ambient temperatures is identical for both AC and heater operations. The heater's electric power demand is almost twice that of the AC because the electric power demand of the AC's compressor is equal to the required cabin cooling power divided by the coefficient of performance (COP) of the refrigeration cycle. By means of an optimal charge management, there is a possibility to replace the precious electric energy used for heating purposes by the free engine warmth. In other words, the longer the engine is kept warm enough to operate the heater, the lower is the power demand of the vehicle. Therefore, an integration between the charge management strategy and engine thermal management is required to achieve the optimal EMS for PHEVs.

The original contribution of this paper is related to the field of EMS of PHEVs and includes the development of a globally optimized EMS based on dynamic programming (DP). It investigates the effect of temperature on the optimal charge depletion trajectory of PHEVs for a predefined journey. The optimal charge trajectory coincides with an engine temperature trajectory which guarantees the optimal engine operation and maximum availability of engine's hot water for cabin heating while satisfying the complete charge depletion constraint. In addition, a practical approach to employ the optimal charge trajectory for calibrating a real-time rule based EMS is presented. Simulations are conducted to present the potential improvements in both fuel efficiency and emissions.

The paper is organized as follows. Section 2 describes the modelling of the vehicle and presents a thermal model of engine. Section 3 describes the numerical optimization method adopted in this work. Section 4 presents the simulation results and associated discussions. Finally, Section 5 provides concluding remarks.

2. Vehicle modelling

A model of EREV is developed with serial powertrain architecture in Advanced Vehicle Simulator (ADVISOR). ADVISOR was written in Matlab/Simulink environment and developed by National Renewable Energy Laboratory (NREL) [19]. The basic characteristics of the vehicle are given in Table 1. Fig. 1 illustrates the main components of the vehicle. It is tried to keep the sizing of the components similar to the published characteristics of GM Volt. GM Volt is a 64 km EREV benefiting from a mode changing architecture by means of a planetary gear set which can shift the vehicle architecture from serial to a series-parallel. In this mode, the engine could mechanically transfer power to the final drive in higher speeds and power demands. Also, it has two different EV modes in which the EV mode shifts from one electric motor drive to two electric motor drives in order to reduce the losses in higher speed and cruise operation [20]. These mode shiftings are not considered in the model of the vehicle used in this paper because the aim of this research is merely the investigation of the effect of temperature on charge management of PHEVs which can be applied to all EREVs regardless of their drivetrain architecture.

Table 1
Powertrain model specifications.

Vehicle	Type:	Small
	Weight:	1700
Engine	Type:	Petrol, 4 cylinder
	Displacement	1 lit
	Maximum Power	41 kW @ 5700 rpm
	Peak Torque	81 Nm @ 3477 rpm
Motor/Generator1	Type:	AC induction
	Maximum Power	124 kW
Motor/Generator2	Maximum Power	54 kW
Battery Pack	Chemistry	Li-Ion
	Nominal Voltage of a Cell	10.67
	Nominal Capacity	6 Ah
	Number of Cells in series	25
	Number of module in Parallel	10
	Pack Energy Capacity	16 kWh

Both cabin and engine thermal models are required to investigate the effect of temperature on both power demand and also engine performance. To predict the power demand of AC and heather, the lumped method for cabin mass, m_{cabin}, and specific heat capacity, $C_{p-\text{cabin}}$, is considered. The energy balance for cooling, Eq. (1), and heating, Eq. (2), should be solved for the cabin control volume to derive the AC/heater loads. Positive direction of heat transfer is selected towards the cabin.

$$m_{\text{cabin}}C_{p-\text{cabin}}\frac{dT_{\text{cabin}}}{dt} = \dot{Q}_{\text{metabolic}} + \dot{Q}_{\text{radiation}} + \dot{Q}_{\text{convection}} + \dot{Q}_{\text{ventilation}} + \dot{Q}_{\text{dehumidification}} - \dot{Q}_{\text{evaporator}} \quad (1)$$

$$m_{\text{cabin}}C_{p-\text{cabin}}\frac{dT_{\text{cabin}}}{dt} = \dot{Q}_{\text{metabolic}} + \dot{Q}_{\text{radiation}} - \dot{Q}_{\text{convection}} - \dot{Q}_{\text{ventilation}} + \dot{Q}_{\text{heater}} \quad (2)$$

The trajectory of an AC/heater power demand in this research is assumed constant. It is possible to predict them by using the energy balance equations Eq. (1) and Eq. (2) based on the method described in authors' previous works [13,21]. Cold-to-hot engine fuel and emissions penalties for SI engines have been investigated by Murrell and Associates [22]. The correction factor has been incorporated based on normalised engine temperature factor, γ, which is related to the engine cooling system's thermostat set point, $T_{\text{Eng}_{\text{tstat}}}$, and the coolant temperature, T_{coolant}:

$$\gamma = \frac{T_{\text{Eng}_{\text{tstat}}} - T_{\text{coolant}}}{T_{\text{Eng}_{\text{tstat}}} - 20} \quad (3)$$

where temperature is in degrees centigrade. The fuel and emissions are then computed based on, γ, and engine performance in hot operation, as follows:

$$\text{Cold Use} = \text{Hot Use} * \text{Cold\_factor} \quad (4)$$

where

$$\text{Cold\_factor} = \begin{cases} (1+\gamma^{3.1}) & \text{fuel} \\ (1+7.4\gamma^{3.072}) & \text{HC} \\ (1+9.4\gamma^{3.21}) & \text{CO} \\ (1+0.6\gamma^{7.3}) & \text{NO}x \end{cases}$$

In case the complete efficiency map of an engine is available for different operation temperatures, it is possible to use lookup tables instead of the abovementioned formulation. The only required temperature to define the cold-factor penalty is the coolant temperature which is assumed to be equal to the internal engine temperature, T_i. A multi node lumped-capacitance thermal network model, depicted in Fig. 2, is defined for the engine thermal model. The generated heat in the engine cylinder, considering the part removed via exhaust, is dissipated among the thermal model nodes based on the heat transfer equations listed in Appendix A.

3. Energy management strategy

As explained in the introduction section, an intelligent charge management as a part of the EMS is required to get the maximum

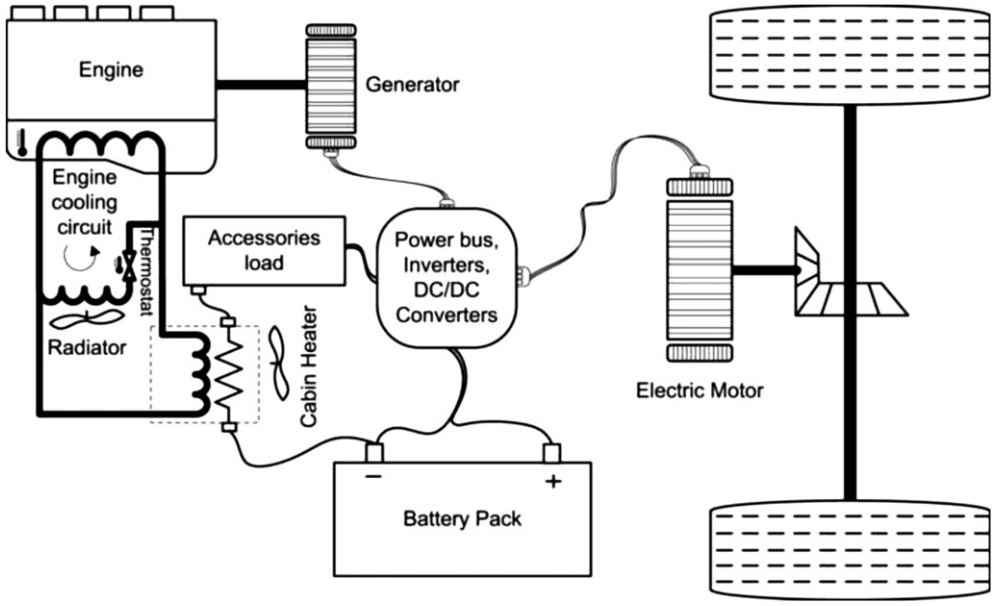

Fig. 1. Schematic of the serial EREV components with a combined electric/engine-coolant cabin heater.

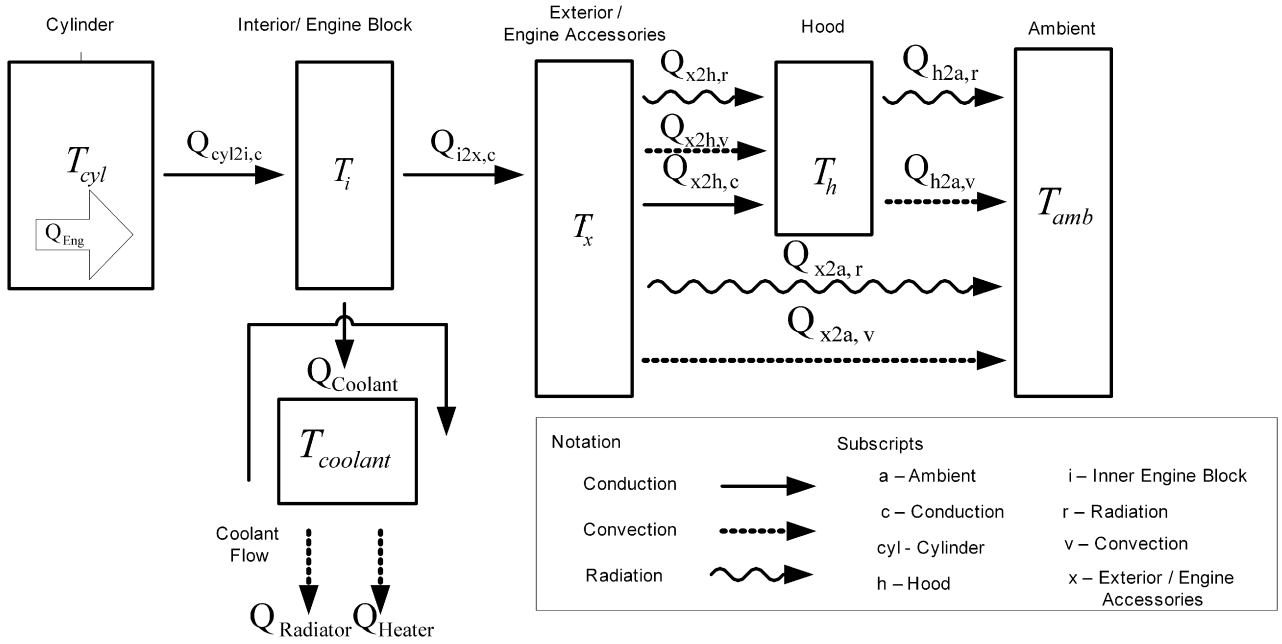

Fig. 2. Schematic illustration of the engine thermal model.

benefits out of the energy stored in the PHEV's ESS. Dynamic programing (DP) is a globally optimal approach which can find the best charge depletion profile, also can act as the benchmark solution for PHEVs' online EMSs. It represents the best possible solution of the control problem with respect to the used discretization of time, state space, and inputs. The biggest disadvantage is the high computational effort which is opposed to a real-time implementation for the online control of a vehicle [11,23–25]. With an acceptable estimate of power cycle, however, DP can help find the optimal charge depletion trajectory for a known driving pattern. That is, DP could be run off-line before the journey starts to find the best SOC and engine temperature trajectories, and also to calibrate the real-time EMS of PHEV. Using external sources via cloud-computing could be a feasible solution to overcome this computational burden. The online approaches like equivalent consumption minimization strategies (ECMS), model predictive control, stochastic dynamic programming, and heuristic strategies are locally optimal approaches which cannot predict the optimal charge depletion strategy and engine thermal management, accordingly.

An inverse powertrain model analogous to the ADVISOR model of the PHEV is formulated as an optimal control problem in dynamic programming to find the optimal charge depletion trajectory and EMS of the PHEV. Based on the principle of optimality suggested by Bellman, the optimal path from any of its intermediate steps to the final states corresponds to the terminal part of the entire optimal solution [2,5,11,26,27]. In the discrete time format:

$$x_{k+1} = f(x_k, u_k) \tag{5}$$

where x_k is the state vector and u_k is the vector of control variables. Here, for the series powertrain architecture, the states are the battery charge, Ch, and the engine internal temperature, T_i, and the control vector is the engine power, P_{Eng}. Electric power equilibrium at the power bus, described in Fig. 1, could be expressed in the form of Eq. (6). Power cycle, the right side of Eq. (6), consists of the electric motor power, P_M, and accessories loads, $P_{Accnohtr}$, and the heater power demand, P_{htr}. When the engine is warm enough, $T_i \geq T_{htr}$, the heater's power demand, P_{htr}, could be supplied by the engine's waste heat.

$$P_{ESS} + \eta_{Gen} \cdot P_{Eng} = P_M + P_{Acc_{nohtr}} + \begin{cases} P_{htr} & T_i < T_{htr} \\ 0 & T_i \geq T_{htr} \end{cases} \tag{6}$$

where P_{ESS}, η_{Gen}, P_{Eng} are ESS power, generator efficiency, and engine power respectively.

It is assumed that the resistance of the battery is independent of the SOC of the battery which is in accordance with $LiFePO_4$ chemistry [25]. Assuming that the ESS model is a perfect open circuit voltage source in series with an internal resistance, and using Eq. (6), the relation between the state, Ch, and the input variable P_{Eng}, is described by :

$$I = \frac{U_0}{2R} - \sqrt{\left(\frac{U_0}{2R}\right)^2 - \frac{P_M + P_{Acc_{nohtr}} + \begin{cases} P_{htr} & T_i < T_{htr} \\ 0 & T_i \geq T_{htr} \end{cases} - \eta_{Gen} \cdot P_{Eng}}{R}} \tag{7}$$

$$\Delta Ch = \Delta t \times I$$

where I, U_0, and R are the battery current, open circuit voltage, and internal resistance respectively.

The internal engine temperature state, $T_i(k)$, is dependent to input variable, P_{Eng}, with heat transfer equations listed in the Appendix A.

The optimization problem in discrete format is to find the control input, u_k, to minimize a cost function (Eq. (7)) which represents fuel consumption from the initial time, t_0, and states, $Ch(t_0)$, $T_i(t_0)$, to the final time, t_f, and states, $Ch(t_f)$, $T_i(t_f)$.

$$\underset{\substack{x \in X \\ u \in U}}{J} = \sum_{k=0}^{t_f - 1} L[x(k), u(k)] = \sum_{k=0}^{t_f - 1} \text{fuel}(T_i(k), P_{Eng}(k)) \tag{8}$$

where L is an instantaneous cost which is hereby defined as fuel consumption. It is possible to add emission and its correspondent weighting factor to the cost function. X and U are respectively admissible PHEV states and control inputs which are defined based on the operational restrictions of battery and engine-generator.

The engine-generator operation is independent of the vehicle speed in the series HEVs' architecture. Therefore, the engine-generator could operate over its optimal operation point for any required power. The combination of these optimal operation points defines a line in engine-generator brake specific fuel consumption (BSFC) map called confined optimal operation line (COOL). In the dynamic programming initialization phase, the heater power demand can be supplied by either engine waste heat or electricity. Accordingly, two corresponding change of charge against fuel consumption cost functions, $\Delta Fuel_{htr}(k, \Delta Ch)$, $\Delta Fuel_{nohtr}(k, \Delta Ch)$, are calculated for each time step by using COOL, Eq. (6), and power cycle. $\Delta Fuel_{htr}(k, \Delta Ch)$ and $\Delta Fuel_{nohtr}(k, \Delta Ch)$ define instantaneous cost for any possible change in the state variable, Ch(k), regardless of second state variable, $T_i(k)$.

By implementing a forward DP approach, a cost-to-go matrix, J, is defined recursively from the initial time-step via discretizing charge of battery and time defined by the duration of drive-cycle. loops for calculation of the cost-to-go matrix to the irregular hexagon showed in schematic cost-to-go matrix in Fig. 3.

In summary, only all possible paths from initial to final SOC are investigated instead of finding the cost-to-go matrix for all discretised charges and times. This could significantly reduce the calculation time for large batteries and for drive-cycles longer than the AER of PHEVs. The Bellman's recursive equation, Eq. (9), is solved by an interpolation method to find the minimum cost to reach a specific node from all possible charges of the previous time step considering both minimum engine-on-time and cold-factor. Cold-factor relates the cost function to the second state variable, $T_i(k)$, using Eq. (4). Also, minimum engine-on-time defines the minimum duration that the engine is permitted to turn off again after it starts. This prevents excessive transient operation of the engine which is generally associated with low efficiency and high emission. All possible charges, $\overrightarrow{Ch}$, costs, $\overrightarrow{j}$, and fuel consumptions, $\overrightarrow{\Delta fuel_{htr}}$ and $\overrightarrow{\Delta fuel_{nohtr}}$, are shown in vector format in Eq. (9).

$$J(k,Ch)=\begin{cases} min\left(\overrightarrow{J}(k-1,\overrightarrow{ch})+\text{Cold\_factor}(k-1,\overrightarrow{ch})\cdot\overrightarrow{\Delta fuel_{htr}}(k-1,\overrightarrow{ch})\cdot\Delta t_{k-1,k}\cdot\begin{cases} inf & ch=1\ and\ t_{eng_{on}}(k)\langle min\_eng\_on \\ 1 & ch\neq 1\ or\ t_{eng_{on}}(k)\geq min\_eng\_on\end{cases}\right) & T_i(k)\langle T_{htr} \\ min\left(\overrightarrow{J}(k-1,\overrightarrow{ch})+\text{Cold\_factor}(k-1,\overrightarrow{ch})\cdot\overrightarrow{\Delta fuel_{nohtr}}(k-1,\overrightarrow{ch})\cdot\Delta t_{k-1,k}\cdot\begin{cases} inf & ch=1\ and\ t_{eng_{on}}(k)\langle min\_eng\_on \\ 1 & ch\neq 1\ or\ t_{eng_{on}}(k)\geq min\_eng\_on\end{cases}\right) & T_i(k)\geq T_{htr}\end{cases} \tag{9}$$

Any node on the cost-to-go matrix represents the minimum cost to reach that specific charge and time from the beginning of the journey. The initial and final charges, as well as the maximum and minimum change of charge in each time step, derived from Eq. (6), are used to determine the possible maximum and minimum charges of each time step. This reduces dimensions of the recursive

The engine on-time, t_{engon}, defining duration of engine operation, and the engine internal temperature, T_i, derived from the thermal model of the engine, are also calculated and saved for each node. Two inequality functions in Eq. (9) define the condition for supplying the heater power demand by the engine waste heat and prevent the engine to turn off before minimum engine-on-time

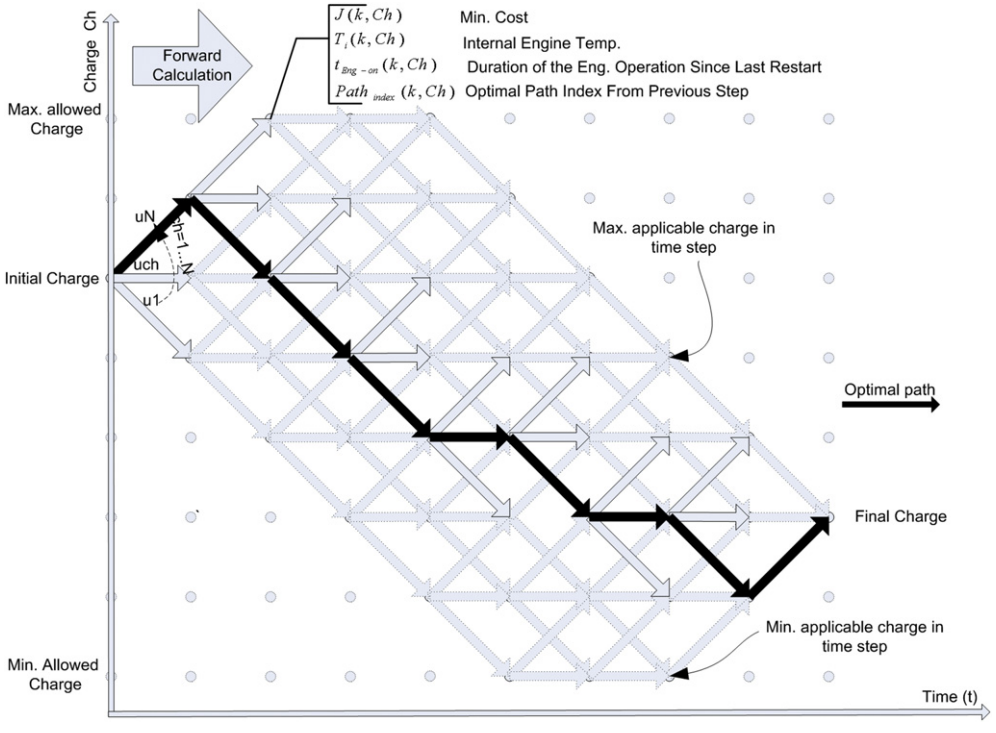

Fig. 3. Graphical representation of cost-to-go matrix.

threshold. For each node of the cost-to-go matrix, the index of the ascendant node defining the optimal path to the specific node is also saved. This is required to identify the initial conditions for cost, $\overrightarrow{J}(k1, \overrightarrow{ch})$, thermal model, $T_i(k-1)$, engine on time, $t_{engon}(k-1)$ for forward cost-to-go calculations and also to find the SOC trajectory in the backward phase of DP. There are two main reasons that make it necessary to use forward instead of backward DP. First, the initial conditions at the end of the journey are unknown, thus the thermal model equations cannot be solved backward. In addition, when the coolant reaches the thermostat temperature, $Q_{Radiator}$, an extra unpredictable unknown is added if the thermal model is to be solved backward. After completion of the forward approach, in the backward calculation stage, optimal charge, temperature, fuel consumption, and engine power trajectories are calculated. The flowchart of the DP code is shown in Fig. 4. The calculation of each time step charge limits and vectorization of the algorithm have improved the performance of the code and simulation time for PHEV battery size and long drive-cycles.

4. Simulation results and discussion

To prove the significance of temperature on the optimal EMS of PHEVs, two 80 km driving scenarios simulating warm and chilly days are defined. Simulations conducted to find the optimal battery charge and its corresponding engine power trajectories using the developed DP code. The results are compared against those of the AER-CS and DP EMS methods which neglect the cold-factor, engine cold start, and heater/AC power demands. The name "DP with cold-factor" is selected for the dynamic programming method described in Section 3. The formulation of "DP without cold-factor" is similar, but does not consider the engine temperature as a state variable in the control problem. Therefore, for the "DP without cold-factor", the cost function in Eq. (9) is defined without considering the cold-factor and the heater power demand inequality function. The drive-cycle represents a typical work-home commute which starts in a suburban area, characterized by UDDS, then continues on a highway, simulated by HWFET, and finally arrives to downtown urban area, UDDS. Destination elevation is around 400 m higher than the starting point. For the warm day driving scenario, vehicle stops during working hours and the engine cools down to the ambient temperature. The return journey is the mirror of the defined driving scenario but the acceleration and deceleration are kept identical. The drive-cycle of both chilly and warm days is similar, yet to show the significance of the heater power demand regardless of the effect of cool-down period in the middle of the journey, a continuous 80 km journey without a cool-down period is simulated. 1.5 kW power demand and COP of 2 for AC refrigeration cycle are assumed for the warm day; therefore, for a similar 10 K difference between cabin comfort, 20 °C, and ambient temperatures, the heater's power demands is defined as 3 kW for the chilly day. The initial power surge and fluctuations during journey are neglected. The simulation results for the warm and chilly days are depicted in Fig. 5 and Fig. 6 respectively and the fuel consumption information is given in Table 2.

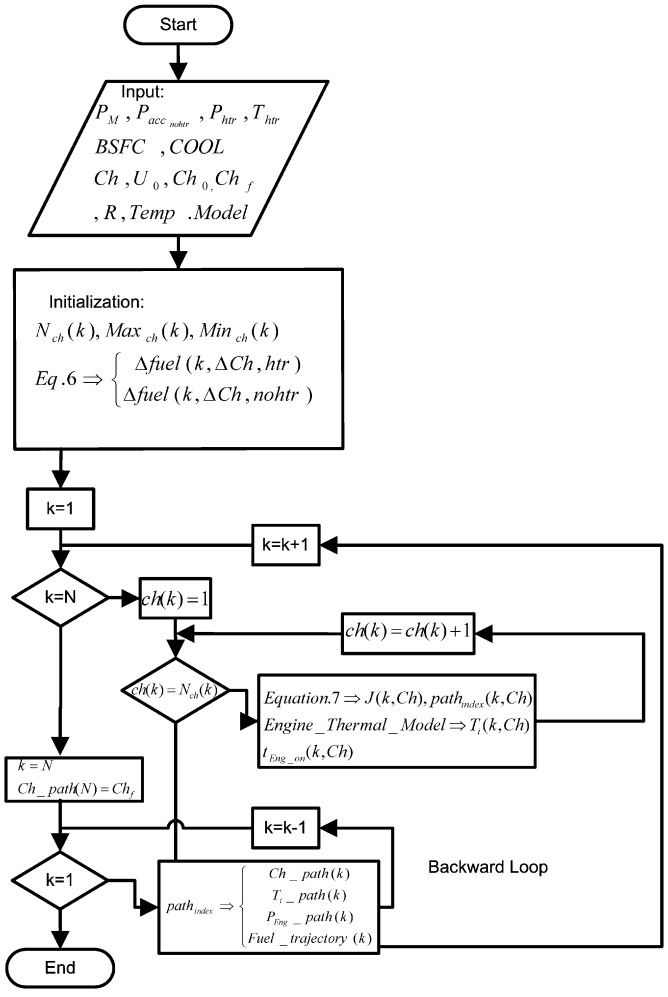

Fig. 4. Flowchart of dynamic programming code.

Fig. 5 demonstrates the simulation results of three EMSs for the warm day commute over the drive-cycle and elevation profile depicted in Fig. 5 (A). "AER-CS", blended mode "DP without cold-factor", and blended mode "DP with cold-factor" are three different EMSs which are compared in this simulation. The corresponding power cycle of the journey is shown in Fig. 5 (B). The engine power trajectory for the AER-CS simulation is illustrated in Fig. 5 (C). During AER, the engine is maintained off until charge sustain time, t_{CS}, when the battery charge reaches minimum applicable SOC. To have a fair comparison with other blended mode EMSs, the DP without cold-factor is used to find the engine power trajectory during the CS mode only for the period of t_{CS} to t_f. Therefore, while the result is optimal for only the CS duration, it would not be a global optimal solution for the whole journey.

The restriction of having the AER at the beginning of the journey is released to develop a blended mode EMS. The DP without cold-factor is employed for the whole journey; hence the engine power trajectory follows the profile illustrated in Fig. 5 (D). The DP without cold-factor finds the global optimal solution for the control problem if it is assumed that the hot engine efficiency is acceptable. Due to the elevation profile, the vehicle power demand is generally lower in return section of the journey. The DP without cold-factor, unlike the AER-CS, allocates most of the battery energy to the return journey and selects the engine-on sections where wheel power demand is generally higher. Therefore, power recirculation is prevented by supplying the wheel power demand directly from the engine instead of recharging the battery when power surplus is available. Although similar code is used for both the CS section and the DP without cold-factor EMS simulations, the fuel consumption is reduced by around 2% via the global optimal charge management. That is, the blended mode EMS allocates batteries' electric energy more efficiently than the AER-CS which consumes all of the batteries' energy during AER.

The engine coolant temperature trajectories shown in Fig. 5 (G) prove that the hot engine operation is not an accurate assumption for EREVs in which the battery supplies significant share of vehicle required energy. This requires modification in DP formulation to

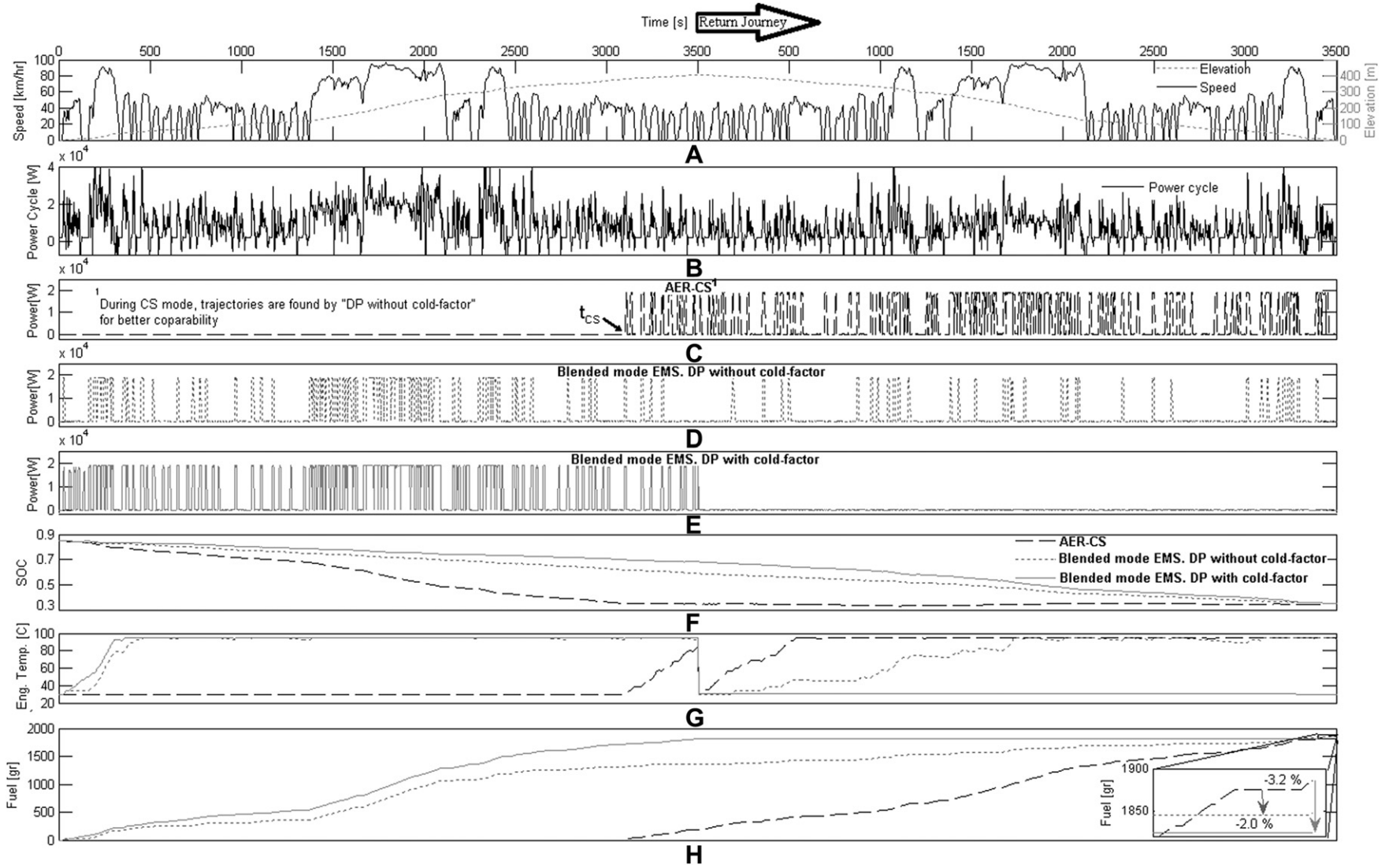

Fig. 5. Simulation results for a warm day with 1.5 kW constant AC power demand and cool-down period at $t = 3500$ (A) drive cycle and elevation profile, (B) power cycle, (C) engine power trajectory of AER-CS EMS, (D) engine power trajectory of blended mode EMS by DP without cold-factor, (E) engine power trajectory of blended mode EMS by DP with cold-factor, (F) battery SOC trajectories, (G) engine coolant temperature trajectories, and (H) fuel consumption trajectories.

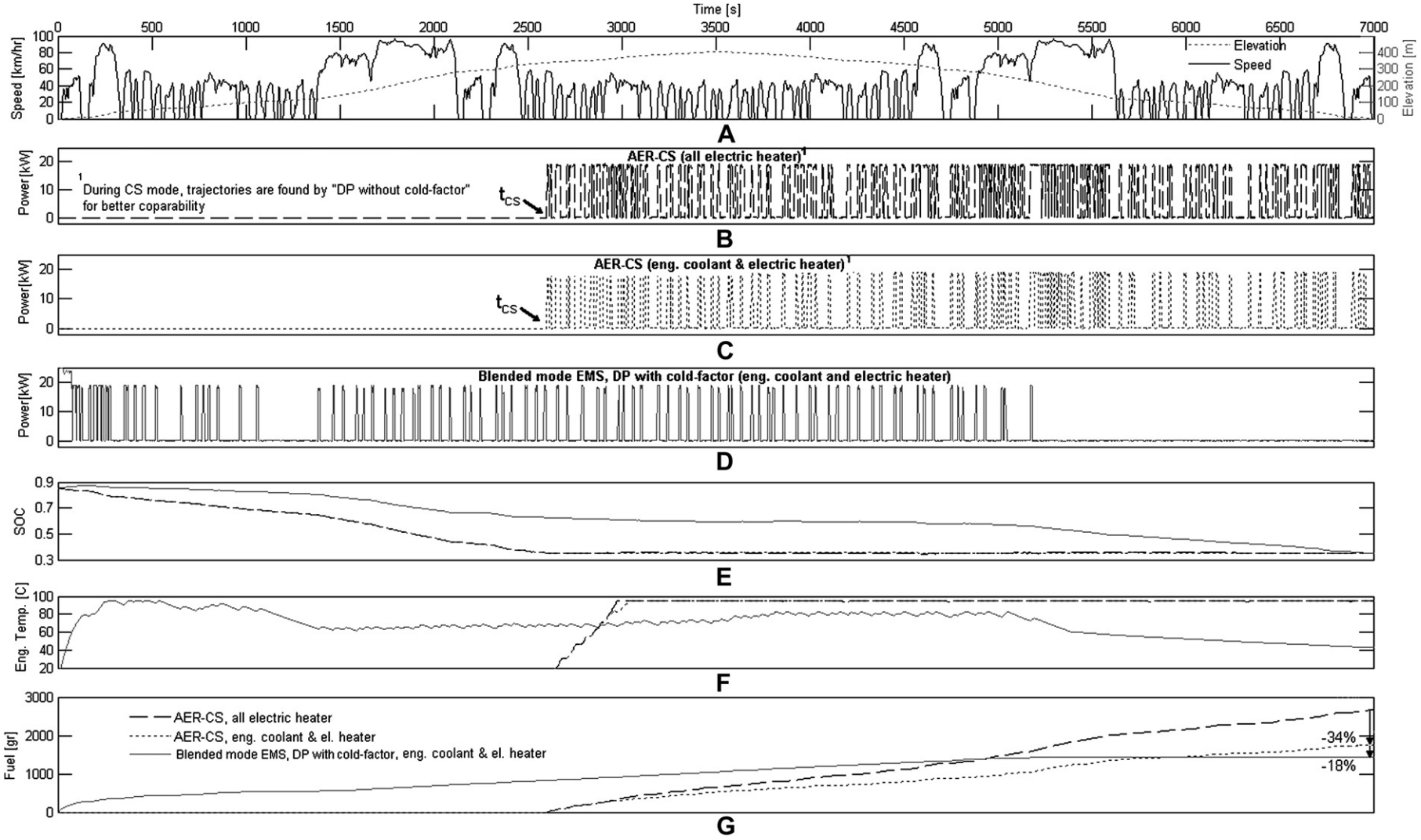

Fig. 6. Simulation results for a chilly day with 3 kW constant heater power demand without a cool-down period (A) drive cycle and elevation profile, (B) engine power of AER-CS EMS of a vehicle with all electric heater (C) engine power of AER-CS EMS, heater power demand is supplied by engine waste heat if $T_i > 60\ ^\circ C$ (D) engine power of CD EMS with cold-factor and heater power demand, heater power demand is supplied by engine waste heat if $T_i > 60\ ^\circ C$ (F) coolant temperature trajectories (G) fuel consumption trajectories.

Table 2
DP and ADVISOR simulation results for warm and chilly days.

		Fuel consumption	HC [g km^{-1}]	CO [g km^{-1}]	NO_x [g km^{-1}]	Engine efficiency	Final SOC
DP Simulation warm day	AER-CS	1885.4 [g]	N.A.	N.A.	N.A.	N.A.	0.35
	1) DP without clod-factor	1847.3 [g]	N.A.	N.A.	N.A.	N.A.	0.35
	2) DP with cold-factor	1824.5 [g]	N.A.	N.A.	N.A.	N.A.	0.35
	Improvement (case 1 compared to AER-CS)	−2.0[a] [%]	N.A.	N.A.	N.A.	N.A.	0
	Improvement (case 2 compared to AER-CS)	−3.2 [%]	N.A.	N.A.	N.A.	N.A.	0
ADVISOR Simulation warm day	AER-CS	2137.8 [g]	0.100	0.379	0.179	0.301	0.346
	Blended EMS, following DP with cold-factor charge trajectory	2010.0 [g]	0.073	0.336	0.148	0.309	0.349
	Improvement/change	−6.0 [%]	−27 [%]	−11.4[%]	−17.3[%]	2.5 [%]	0.9 [%]
DP Simulation chilly day	1) AER-CS All electric heater	2667.2 [g]	N.A.	N.A.	N.A.	N.A.	0.35
	2) AER-CS both engine coolant and electric heater	1754.7 [g]	N.A.	N.A.	N.A.	N.A.	0.35
	DP with cold-factor	1434.4 [g]	N.A.	N.A.	N.A.	N.A.	0.35
	Improvement (DP compared to case 1)	−34.2 [%]	N.A.	N.A.	N.A.	N.A.	0
	Improvement (DP compared to case 2)	−18.3 [%]	N.A.	N.A.	N.A.	N.A.	0
ADVISOR Simulation chilly day	1) AER-CS All electric heater	2784.8 [g]	0.162	0519	0.194	0.307	0.349
	2) AER-CS both engine coolant and electric heater	1892.6 [g]	0.139	0.440	0.142	0.298	0.350
	Blended EMS, following DP with cold-factor charge trajectory	1628.4 [g]	0.136	0.415	0.132	0.289	0.354
	Improvement/change (Blended EMS compared to case 1)	−41.5 [%]	−16.1[%]	−20.0[%]	−32.0[%]	−5.9 [%]	1.4 [%]
	Improvement/change (Blended EMS compared to case 2)	−13.9 [%]	−2.2 [%]	−5.7 [%]	−7.0 [%]	−3.0 [%]	1.1 [%]

[a] The negative sign (−) means reduction in fuel consumption and emission.

consider effect of temperature as a state variable which is explained in Section 3. Employing the DP with cold-factor, the EV mode completely shifts to return journey and all engine-on sections are concentrated before the cool-down period. This eliminates the second cold start warm-up procedure which leads to cold engine operation and consequently the cold-factor penalty. The DP with cold-factor selects the first section of the commute for the blended mode operation, as the batteries' energy is adequate to run the downhill return journey in the EV mode. The overall engine efficiency for the whole journey is higher when one extra engine warm-up is eliminated. That is, the effect of warmer engine operation overcompensate the reduction of vehicle efficiency because of the engine operation in the lower power demand when compared with the DP without cold-factor. Our proposed "DP with cold-factor" approach improves the fuel economy of the vehicle by 3.2% compared with the AER-CS EMS. Therefore, it improves the performance of the DP without cold-factor by 1.2%. This result simulates inaccuracy of relying on the DP without cold-factor for PHEVs with large batteries as the optimal EMS benchmark. In addition, as described in the introduction section, the cold operation of the engine and catalyst converter has a major role in the emission of the vehicle. Therefore, the environmental impact of the emission reduction by elimination of the second cold-start may outweigh the amount of fuel saved. According to the simulation conducted in ADVISOR, the HC, CO, and NOx emissions are reduced by almost 27%, 11%, and 17% respectively compared to the AER-CS simulation (see Table 2).

The engine operation trajectories of the AER-CS EMS of a full electric cabin heater vehicle and a vehicle in which the heater power is supplied by both the batteries and the engine waste heat are compared in Fig. 6 (B, C). The significant 34% improvement in the fuel economy could be realized by employing the waste heat of the engine like conventional vehicles. Based on the authors' knowledge gained at 2011 Frankfurt motor show, the GM Volt cabin heater is an all-electric, while Opel has solved the issue for the Ampera models. The engine power path shown in Fig. 6 (D) is derived based on the DP EMS with cold-factor for a vehicle with both engine coolant and electric heater. Fig. 6 (F) illustrates how the optimal EMS found by the DP with cold-factor tends to keep the engine warm for longer duration to provide the cabin heater's power demand free of cost. Indeed, holding the temperature not exactly at the thermostat temperature comes at a cost of reduction in engine efficiency defined by the cold-factor. The optimal EMS based on DP compromises between maximum availability of the hot water from the engine by distributing engine-on sections during the journey and the effect of cold-factor on the engine efficiency. Referring to Table 2, for ADVISOR simulation, 14% improvement in the fuel economy is achieved, while the engine efficiency is reduced by 3% because of the operation at temperatures below thermostat set-point. That is, the amount of fuel saved by keeping the engine warm outweighs the drawback of its operation at not exactly the thermostat temperature set-point. When heater operation is required for cold weather, DP with cold-factor method finds the optimal trajectory of state variables, ESS charge and accordingly the engine internal temperature, to minimize the fuel consumption cost function. It is interesting how the optimal method still selects a short EV mode at the end of the journey. Since the energy demand of the heater is directly related to the duration of the journey, as well as the ambient temperature, its influence on the optimal EMS of PHEVs is more significant for cold weather, long journeys, and especially for low power demand city drive-cycles. Although the wheel power demand of the vehicle in both simulations of warm and chilly days is similar, the final optimal charge depletion and EMS for different temperatures and AC/heater power demands are significantly different. The warm day simulation shows how a cold-factor might affect the optimal EMS to concentrate engine operation before the cool down period for the defined driving scenario. On the other hand, the combination of effect of cold-factor and desirability of keeping the engine warm for cabin

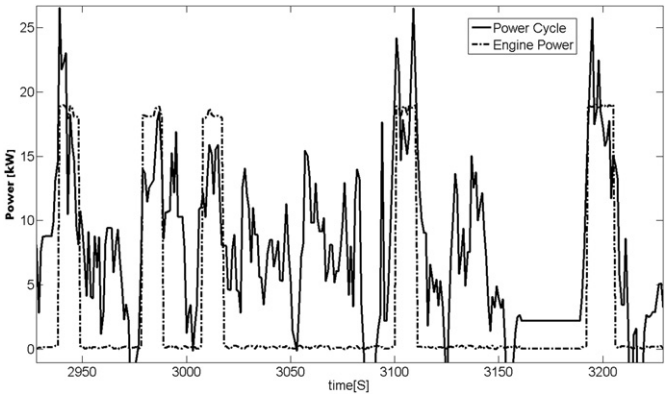

Fig. 7. A superimposed selected section of Fig. 5. (B) and (D).

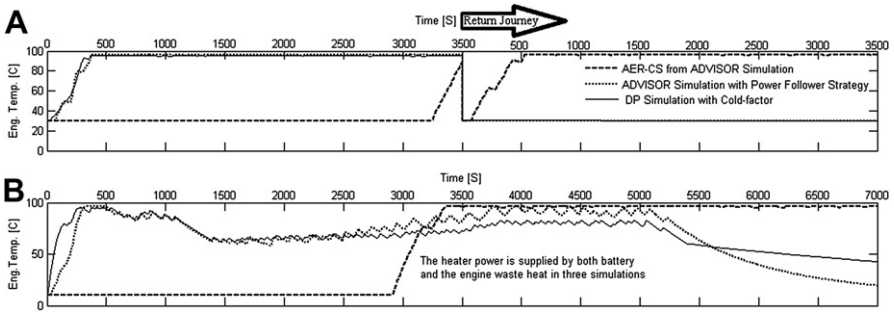

Fig. 8. (A) Comparison of the coolant temperature trajectories in ADVISOR and DP with cold-factor simulations for (A) Warm day (B) Chilly day.

heater purpose distributes the engine operation sections throughout the journey for the chilly day simulation. While for warm weather operation keeping engine temperature close to thermostat temperature is the dominant parameter to achieve optimal overall efficiency, for the chilly day simulation, the availability of hot water for cabin heater dominates to avoid electric heater operation.

Simulations also show another interesting result that the engine power has limited fluctuations around the most efficient engine operation point regardless of changes in the power demand (see Fig. 7). This implies that the optimal operation of the vehicle dominantly depends on the engine efficient operation. Since the large PHEV's ESS benefits from parallel modules, its internal resistance compared to the conventional HEVs is significantly lower. Therefore, the electrical waste in PHEV's ESS is reduced accordingly.

5. Real-time implementation

Although the DP approach could not be implemented in a real-time control of vehicle, the optimal charge depletion trajectory for a known driving scenario could help calibrate the EMS in an online fashion. That is, the real-time EMS tries to implement the same optimal charge management by following the charge trajectory found by the DP approach. Particularly, the DP approach can suggest the best sections of the journey to run on the pure EV mode for EREV. The charge trajectory should be followed based on position feedback of vehicle in a journey instead of time domain using the GPS. In the following, it is described how effectively only the knowledge of optimal charge trajectory regardless of type of real-time EMS could significantly improve the performance of PHEV.

The well-known rule based power follower EMS controls the vehicle in ADVISOR simulation tool for the same driving scenario explained in the previous section. (See Appendix B for the list of rules). The ADVISOR model is manipulated to simulate the heater and AC loads and effect of heater cool-down on engine thermal model. Also, the vehicle control unit is redesigned to sustain the ESS SOC around charge depletion trajectory derived from the DP approach by using a feedback control. The results are shown in Fig. 8 and Table 2. The engine power trajectories of the DP and the power follower ADVISOR model are completely different in terms of details. By following the charge trajectory found by DP with cold-factor, however, the batteries to engine energy ratio during the journey is remained similar to the DP optimal trend. This results in almost similar engine temperature trajectory. The slight deviation between the temperature trajectories of DP with cold-factor and ADVISOR simulations is a result of the difference between the engine operation trajectories and also the difference between the heater cooling effect on engine thermal model of the DP and ADVISOR. Due to discretization, the heater power demand is defined step-wise for the DP model which shifts at a defined threshold. Yet, the heater cooling effect on engine thermal model of ADVISOR is defined by a linear equation so the cooling effect continues for all temperatures (see Appendix A).

The amount of fuel saved for the chilly day simulation proves the significant drawback of using only electric heater. Improvement in fuel efficiency of vehicle could be even considerably increased for extreme low temperatures. Besides, the emission reduction is another positive aspect of an EMS considering temperature noise factor; particularly, when an unnecessary cold-start/warm-up of the engine and catalytic converter is eliminated.

6. Conclusion

The significance of temperature noise factor on optimal energy management strategy of Plug-in Hybrid Electric Vehicles is demonstrated in this paper via using a Dynamic Programming approach. DP based on Bellman's principle of optimality derives optimal charge depletion trajectory of the battery. This coincides with the optimal thermal management of the engine for minimum fuel consumption, while maximizing employing engine waste heat for cabin warming instead of the battery electricity. The simulation results prove that temperature considerably changes the optimal EMS and accordingly fuel consumption and emission of PHEVs even for identical drive cycles. A practical approach to implement the result of the optimal EMS for calibrating a real-time EMS which addresses the realistic disturbances of real world driving is also proposed.

Nomenclature

AC	air condition
AER	all electric range
BSFC	brake specific fuel consumption
Ch	battery charge
COOL	confined optimal operation line
COP	coefficient of performance
CS	charge sustained mode
C_p	thermal heat capacity
DP	dynamic programming
ECMS	equivalent consumption minimization strategies
Eng	engine
EMS	energy management strategy
EREV	extended range electric vehicle
ESS	energy storage system
EV	electric vehicle
fuel	fuel
Flw	flow rate
GIS	geographical information system
GPS	global positioning system
h	heat transfer coefficient
HEV	hybrid electric vehicle
HWFET	highway fuel economy test
I	battery current

inf	infinity
J	cost function
k	index for time discretization
L	instantaneous cost
lhv	fuel lower heating value
m	mass
$\dot{m}$	mass flow rate
min_eng_on	minimum engine on time
N	number of possible change of charge in each time-step
PHEV	plug in hybrid electric vehicle
P	engine power
Q	rate of thermal energy
R	battery internal resistance
sarea	surface area
SOC	state of charge
t	time
T	temperature
T_{htr}	temperature threshold for using engine coolant waste heat for cabin heater
u	input variable
U	admissible input variables
U_0	battery nominal voltage
UDDS	urban dynamometer driving schedule
V	velocity
x	state variable
X	admissible state variables
γ	normalized engine temperature
ω	engine angular velocity
σ	Stefan–Boltzmann constant
η	efficiency

Subscripts

air	air
acc	accessories
amb	ambient
c	conduction
coolant	engine coolant
cyl	cylinder
emisv	emissivity factor
Eng	engine
exh	exhaust gas
f	final time
fuel	fuel
Gen	generator
h	hood
Htr	cabin heater
i	engine interior
k	index for time discretization
M	electric traction motor
nohtr	heater is not using electric power
traction	traction
r	thermal radiation
Radiator	radiator
th_c	thermal conduction coefficient
tstat	thermostat set point
x	engine exterior
0	initial time

Appendix A. List of equations used for engine thermal model

$$Q_{Eng} = Q_{fuel} - P_{traction} - Q_{exh} = \dot{m}_{fuel}\cdot lhv - \tau\cdot\omega - \dot{m}_{exh}C_{p,exh}(T_{exh} - T_{amb}) \quad (A.1)$$

$$Q_{cyl2i,c} = Eng_{cyl2i\_th\_c}{}^{*}\left(T_{cyl} - T_i\right) \quad (A.2)$$

$$Q_{i2x,c} = Eng_{i2x\_th\_c}{}^{*}(T_i - T_x) \quad (A.3)$$

$$Q_{Radiator} = \begin{cases} Q_{c2i,c} - Q_{i2x,c} - Q_{Heater} & T_i > Eng_{tstat} \\ 0 & T_i \le Eng_{tstat} \end{cases} \quad (A.4)$$

$$Q_{Htr} = \eta_{Htr}\cdot Flw_{Htr}.C_p\cdot(T_i - T_{amb}) \text{ Advisor Model} \quad (A.5)$$

$$Q_{Htr} = \begin{cases} P_{htr} & T_i \ge T_{htr} \\ 0 & T_i < T_{htr} \end{cases} \text{ DP Model} \quad (A.6)$$

$$Q_{x2h,r} = \varepsilon\sigma^{*}A^{*}\left(T_x^4 - T_h^4\right) = Eng_{emisv}{}^{*}5.67E-8{}^{*}sarea_x{}^{*}\left(T_x^4 - T_h^4\right) \quad (A.7)$$

$$Q_{x2h,v} = h_{air}{}^{*}A^{*}(T_x - T_h) = h_{air}{}^{*}sarea_x{}^{*}(T_x - T_h) \quad (A.8)$$

$$Q_{x2h,c} = Eng_{h2x\_th\_c}{}^{*}(T_x - T_h) \quad (A.9)$$

$$Q_{x2a,r} = \varepsilon\sigma^{*}A^{*}\left(T_x^4 - T_{amb}^4\right) = Eng_{emisv}{}^{*}5.67E-8{}^{*}sarea_x{}^{*}\left(T_x^4 - T_{amb}^4\right) \quad (A.10)$$

$$Q_{x2a,v} = h_{air}{}^{*}A^{*}(T_x - T_{amb}) = h_{air}{}^{*}sarea_x{}^{*}(T_x - T_{amb}) \quad (A.11)$$

$$Q_{h2a,r} = \varepsilon\sigma^{*}A^{*}\left(T_h^4 - T_{amb}^4\right) = Eng_{emisv}{}^{*}5.67E-8{}^{*}sarea_h{}^{*}\left(T_x^4 - T_{amb}^4\right) \quad (A.12)$$

$$Q_{h2a,v} = h_{air}{}^{*}A^{*}(T_h - T_{amb}) = h_{air}{}^{*}esarea_h{}^{*}(T_h - T_{amb}) \quad (A.13)$$

$$h_{air} = 6 + 6^{*}(\Delta T/1000)^{0.25} + 60^{*}(V_{air}/30)^{0.63} \quad (A.14)$$

$$T_c = \int_0^t \frac{Q_{Eng} - Q_{c2i,c}}{m_{Eng,c}{}^{*}C_{p,Eng}}dt \quad (A.15)$$

$$T_i = T_{Coolant} = \int_0^t \frac{Q_{c2i,c} - Q_{Radiator} - Q_{Htr} - Q_{i2x,c}}{m_{Eng,i}{}^{*}C_{p,Eng}}dt \quad (A.16)$$

$$T_x = \int_0^t \frac{Q_{i2x,c} - Q_{x2h,r} - Q_{x2h,v} - Q_{x2h,c} - Q_{x2a,r} - Q_{x2a,v}}{m_{Eng,x}{}^{*}C_{p,Eng}}dt \quad (A.17)$$

$$T_h = \int_0^t \frac{Q_{x2h,r} + Q_{x2h,v} + Q_{x2h,c} - Q_{h2a,r} - Q_{h2a,v}}{m_{Eng,x}{}^{*}C_{p,Eng}}dt \quad (A.18)$$

Appendix B. List of Power follower rule-based EMS implemented in ADVISOR

- Engine may be turned off if SOC is over 1% higher than pre-defined trajectory.

- Engine may be turned on again if the power required by the vehicle gets high enough.
- Engine may be turned on again if SOC is at least 1% lower than predefined trajectory.
- When the engine is on, its power output tends to follow the power required by the vehicle. The engine torque and speed are selected based on the COOL. The engine output power is adjusted tending to bring SOC back to predefined SOC trajectory.
- The engine output power may be kept above some minimum value (6 kW) and below some maximum value (26 kW). The engine output power may be allowed to change no faster than a prescribed rate ($+2$ and -3 kW s^{-1}) and if it turns on it is kept on for at least a prescribed time (10 s).
- During engine-on, the batteries only provides the power shortage required by the vehicle when engine inertia or power follower rate limiter rules cause a difference between the powertrain required power and the engine available power.

References

[1] J. Tollefson, Nature 456 (2008) 436–440.
[2] L. Guzzella, A. Sciarretta, Vehicle Propulsion Systems: Introduction to Modeling and Optimization, second ed., Springer, 2007.
[3] P. Pisu, G. Rizzoni, IEEE Transactions on Control Systems Technology 15 (2007) 506–518.
[4] F.R. Salmasi, IEEE Transactions on Vehicular Technology 56 (2007) 2393–2404.
[5] L. Serrao, A comperative analyses of energy management strategies for hybrid electric vehicles, PhD thesis, The Ohio State University, 2009.
[6] S.G. Wirasingha, A. Emadi, Classification and review of control strategies for plug-in hybrid electric vehicles, in: IEEE Vehicle Power and Propulsion Conference, 2009.
[7] Y. Bin, Y. Li, Q. Gong, Z.-R. Peng, Multi-information integrated trip specific optimal power management for plug-in hybrid electric vehicles, in: American Control Conference, 2009.
[8] Z. Bingzhan, C.C. Mi, Z. Mengyang, IEEE Transactions on Vehicular Technology 60 (2011) 1516–1525.
[9] Y. Gao, M. Ehsani, IEEE Transactions on Industrial Electronics 57 (2010) 633–640.
[10] J. Gonder, T. Markel, Energy management strategies for plug-in Hybrid Electric Vehicles, in: SAE World Congress & Exhibition, 2007.
[11] Q. Gong, Y. Li, Z.-R. Peng, IEEE Transactions on Vehicular Technology 57 (2008) 3393–3401.
[12] S.J. Moura, H.K. Fathy, D.S. Callaway, J.L. Stein, IEEE Transactions on Control Systems Technology 19 (2010) 1–11.
[13] M. Shams-Zahraei, A.Z. Kouzani, B. Ganji, International Review of Electrical Engineering 6 (2011) 1715–1726.
[14] M. Shams-Zahraei, A.Z. Kouzani, Power-cycle-library-based Control Strategy for Plug-in Hybrid Electric Vehicles, in: IEEE Vehicle Power and Propulsion Conference 2010.
[15] P.B. Sharer, A.P. Rousseau, D. Karbowski, S. Pagerit, Plug-in hybrid electric vehicle control strategy: comparison between EV and charge depleting options, in: SAE World Congress & Exhibition, 2008.
[16] G.W. Taylor, S. Stewart, Cold start impact on vehicle energy use, in: SAE World Congress & Exhibition, 2001.
[17] H. Li, G.E. Andrews, D. Savvidis, B. Daham, K. Ropkins, M. Bell, J. Tate, SAE International Journal of Engines 1 (2008) 804–819.
[18] R. Farrington, J. Rugh, Impact of vehicle air-conditioning on fuel economy, tailpipe emissions, and electric vehicle range, in: Earth Technologies Forum, 2000.
[19] T. Markel, A. Brooker, T. Hendricks, V. Johnson, K. Kelly, B. Kramer, M. O'Keefe, S. Sprik, K. Wipke, Journal of Power Sources 110 (2002) 255–266.
[20] M. Miller, A. Holmes, B. Conlon, P. Savagian, The GM "Voltec" 4ET50 Multi-Mode Electric Transaxle in: SAE World Congress & Exhibition, 2011.
[21] H. Khayyam, A.Z. Kouzani, E.J. Hu, S. Nahavandi, Applied Thermal Engineering 31 (2010) 750–764.
[22] J.D. Murrell, Emission Simulations: GM Lumina, Ford Taurus, GM Impact, and Chrysler TEVan, Report by: J. Dill Murrell and Associates, 1996.
[23] A. Brahma, Y. Guezennec, G. Rizzoni, Optimal energy management in series hybrid electric vehicles, in: American Control Conference, 2000.
[24] L. Chan-Chiao, P. Huei, J.W. Grizzle, K. Jun-Mo, IEEE Transactions on Control Systems Technology 11 (2003) 839–849.
[25] S. Kutter, B. Bäker, Predictive online control for hybrids: resolving the conflict between global optimality, robustness and real-time capability, in: IEEE Vehicle Power and Propulsion Conference 2010.
[26] S. Bradley, A. Hax, T. Magnanti, Applied Mathematical Programming, Addison-Wesley Pub. Co, 1977.
[27] D. Kirk, Optimal Control Theory an Introduction Dover Publications, Mineola, New York, 2004.